

## NARC-1/PCSK9 and Its Natural Mutants

ZYMOGEN CLEAVAGE AND EFFECTS ON THE LOW DENSITY LIPOPROTEIN (LDL) RECEPTOR AND LDL CHOLESTEROL\*

Received for publication, August 23, 2004, and in revised form, September 8, 2004  
Published, JBC Papers in Press, September 9, 2004, DOI 10.1074/jbc.M409699200

Suzanne Benjannet,<sup>a</sup> David Rhainds,<sup>a,b</sup> Rachid Essalmani,<sup>a</sup> Janice Mayne,<sup>c</sup> Louise Wickham,<sup>a</sup> Weijun Jin,<sup>d</sup> Marie-Claude Asselin,<sup>a</sup> Josée Hamelin,<sup>a</sup> Mathilde Varret,<sup>e</sup> Delphine Allard,<sup>e,f</sup> Mélanie Trillard,<sup>e</sup> Marianne Abifadel,<sup>e,g</sup> Angie Tebon,<sup>h</sup> Alan D. Attie,<sup>h</sup> Daniel J. Rader,<sup>d</sup> Catherine Boileau,<sup>e</sup> Louise Brissette,<sup>i</sup> Michel Chrétien,<sup>c</sup> Annik Prat,<sup>a</sup> and Nabil G. Seidah<sup>a,j</sup>

From the <sup>a</sup>Laboratory of Biochemical Neuroendocrinology, Clinical Research Institute of Montreal, Montreal, Quebec H2W 1R7, <sup>b</sup>Regional Protein Chemistry Center, Diseases of Ageing Unit, Ottawa Health Research Institute, Ottawa, Ontario K1Y 4E9, Canada, the <sup>c</sup>Department of Medicine, University of Pennsylvania School of Medicine, Philadelphia, Pennsylvania 19104, <sup>d</sup>INSERM U383, Hôpital Necker-Enfants Malades, AP-HP, Université Paris V, 149-161 Rue de Sèvres, 75743 Paris Cedex 15, France, the <sup>e</sup>Department of Biochemistry, University of Wisconsin, Madison, Wisconsin 53706, and the <sup>f</sup>Département des Sciences Biologiques, Université du Québec à Montréal, C.P. 8888, Succursale Centre-Ville, Montreal, Quebec H3C 3P8, Canada

The discovery of autosomal dominant hypercholesterolemic patients with mutations in the *PCSK9* gene, encoding the proprotein convertase NARC-1, resulting in the missense mutations suggested a role in low density lipoprotein (LDL) metabolism. We show that the endoplasmic reticulum-localized proNARC-1 to NARC-1 zymogen conversion is Ca<sup>2+</sup>-independent and that within the zymogen autocatalytic processing site SSVFAQ ↓ SIP Val at P4 and Pro at P3' are critical. The S127R and D374Y mutations result in ~50–60% and ≥98% decrease in zymogen processing, respectively. In contrast, the double [D374Y + N157K], F216L, and R218S natural mutants resulted in normal zymogen processing. The cell surface LDL receptor (LDLR) levels are reduced by 35% in lymphoblasts of S127R patients. The LDLR levels are also reduced in stable HepG2 cells overexpressing NARC-1 or its natural mutant S127R, and this reduction is abrogated in the presence of 5 mM ammonium chloride, suggesting that overexpression of NARC-1 increases the turnover rate of the LDLR. Adenoviral expression of wild type human NARC-1 in mice resulted in a maximal ~9-fold increase in circulating LDL cholesterol, while in LDLR(–/–) mice a delayed ~2-fold increase in LDL cholesterol was observed. In conclusion, NARC-1 seems to affect both the level of LDLR and that of circulating apoB-containing lipoproteins in an LDLR-dependent and -independent fashion.

include the 7 basic amino acid-specific convertases known as PC1/PC3, PC2, furin, PC4, PACE4, PC5/PC6, PC7/LPS (1, 2) and the two enzymes cleaving at nonbasic residues SKI-1/S1P (3, 4) and NARC-1/PCSK9 (5). These proteases are implicated in the limited proteolysis of precursors of secretory proteins that regulate a variety of cellular functions, including cellular growth, adhesion, differentiation, cell to cell communications, and endocrine/paracrine functions (6, 7). Published gene knock-out analyses (reviewed in Ref. 8) revealed that only furin (9) and SKI-1/S1P (10) are embryonic lethal. So far, nothing is known about the phenotype consequences of NARC-1<sup>1</sup> knock-out in mice. The cDNA of the enzyme NARC-1 was cloned during pharmaceutical screening of mRNAs up-regulated following induction of neural apoptosis by serum withdrawal, and the encoded protein was called “neural apoptosis regulated convertase 1” (NARC-1) (11). We characterized this enzyme, and we showed that it is highly expressed in liver and small intestine and that specific mutations in the prosegment of NARC-1 completely abrogated its autocatalytic processing (5). We further showed that overexpression of NARC-1 enhances neurogenesis of progenitor brain telencephalic cells. The sustained expression of NARC-1 in liver and small intestine and its transient expression in telencephalon, kidney, and cerebellum beg for the identification of its physiological substrates, which are still unknown.

Human genetic point mutations resulting in pathology have been reported only for two of the proprotein convertases (PCs), namely PC1 (gene *PCSK1*) (12, 13) and NARC-1 (gene *PCSK9*) (14). Two distinct missense mutations, one on each allele of *PCSK1*, are responsible for a recessive form of obesity (12) and

The mammalian proprotein convertases constitute a family of 9 serine proteinases related to bacterial subtilisin. These

\* This work was supported in part by Canadian Institutes of Health Research Grants MOP 36496 and MOP 44362, Group Grant MGC-64518, and National Institutes of Health Grant HL56593. The costs of publication of this article were defrayed in part by the payment of page charges. This article must therefore be hereby marked “advertisement” in accordance with 18 U.S.C. Section 1734 solely to indicate this fact.

<sup>b</sup> Supported by a Natural Sciences and Engineering Council of Canada fellowship.

<sup>f</sup> Supported by a grant from the Ministère de l'Enseignement Supérieur et de la Recherche, France.

<sup>g</sup> Supported by a grant from the Nouvelle Société Française d'Athérosclérose, France.

<sup>j</sup> To whom correspondence should be addressed: Clinical Research Institute of Montreal, Laboratory of Biochemical Neuroendocrinology, 110 Pine Ave. West, Montreal, Quebec H2W 1R7, Canada. Tel.: 514-987-5609; Fax: 514-987-5542; E-mail: seidah@ircm.qc.ca.

<sup>1</sup> The abbreviations used are: NARC-1, neural apoptosis regulated convertase 1; apoB, apolipoprotein B; ADH, autosomal dominant hypercholesterolemia; HCHOLA3, third locus; ER, endoplasmic reticulum; HEK, human embryonic kidney; LDL, low density lipoprotein; LDLR, LDL receptor; PC, proprotein convertase; SREBP, sterol regulatory element binding protein; SKI-1, subtilisin-kexin isozyme 1; FACS, fluorescence-activated cell sorter; mAb, monoclonal antibody; Tricine, N-[2-hydroxy-1,1-bis(hydroxymethyl)ethyl]glycine; EBV, Epstein-Barr virus; MEM, minimum Eagle's medium; BSA, bovine serum albumin; PBS, phosphate-buffered saline; RT, room temperature; SELDI-TOF-MS, surface-enhanced laser desorption time-of-flight mass spectrometry; FPLC, fast protein liquid chromatography; HDL, high density lipoprotein; WT, wild type; RP, relative processing; EGFP, enhanced green fluorescent protein.

endocrine malfunctions (13). Autosomal dominant hypercholesterolemia (ADH) is a risk factor for coronary heart disease, which is characterized by an increase in low density lipoprotein (LDL) cholesterol levels that is associated with mutations in the genes *LDLR* or *APOB* (15). Three single point mutations in *PCSK9* causing amino acid changes were reported, each genetically linked to a third form of ADH. The mutations S127R or F216L were detected in different French families (14), the mutant D374Y in a large Utah pedigree (16), and in Norwegian subjects (17). In the latter study, one patient exhibited a double mutation D374Y + N157K (17), although it is not clear if both mutations are on the same allele. In all cases, the circulating levels of total cholesterol and LDL cholesterol were 2–6-fold higher than normal. Whereas mutations in the NARC-1 gene *PCSK9* result in a hypercholesterolemic phenotype, nothing is known about the mechanism(s) behind this effect and whether such mutations affect the enzymatic activity of NARC-1 and/or are due to a gain of nonenzymatic function. Recently, the common polymorphic intron 1 (C(-161)T) and exon 9 (I474V) variants in *PCSK9* gene (14) were shown to be significantly associated with increased total cholesterol and LDL cholesterol levels in the general population in Japan (18).

Independently, two groups used microarray technology to study mRNAs that are regulated by cholesterol or the sterol regulatory element binding proteins (SREBPs), and came to the conclusion that NARC-1 is likely to be implicated in sterol/lipid metabolism (19, 20). Furthermore, recent data from our group demonstrated that NARC-1 mRNA levels are up-regulated in hepatocyte-derived HepG2 cells by the hydroxymethylglutaryl-CoA reductase inhibitors “statins.” This process can be reversed by mevalonate treatment, implicating SREBP-2 in the up-regulation of NARC-1 (21). In contrast to NARC-1, the mRNA levels of SKI-1 are not sensitive to cholesterol, despite the fact that it is a key protease in the cleavage of sterol regulatory element-binding proteins (SREBPs) (22, 23). Thus, NARC-1 and SKI-1 participate in the regulated response to intracellular cholesterol levels and LDL metabolism via different mechanisms.

The zymogen proNARC-1 is autocatalytically processed in the endoplasmic reticulum (ER) into NARC-1 that is secreted as a complex with its ~14-kDa prosegment (5). The pro-form of NARC-1 (pro-NARC-1) is found predominantly in the ER (5). In this report we have focused on the zymogen processing of pro-NARC-1 and the secretion of mature NARC-1. This led us to demonstrate that the human natural mutations S127R and especially D374Y greatly reduce the extent of NARC-1 zymogen processing, whereas the F216L, R218S, N157K alone and the double D374Y + N157K mutations do not seem to significantly affect this process. We also show that although NARC-1 does not contain a P-domain, its C-terminal Cys/His-rich domain is important for efficient zymogen processing.

Furthermore, we show that patients with the heterozygote S127R NARC-1 mutation exhibit 35% lower levels of LDLR at the surface of their lymphoblasts, a finding that was reproduced in HepG2 cells overexpressing this mutant, and reversed in the presence of the lysosomotropic agent  $\text{NH}_4\text{Cl}$  (24). Further proof that NARC-1 regulates LDL production comes from the fact that adenoviral expression of human NARC-1 in mice led to a very significant time-dependent increase in circulating LDL cholesterol even in the absence of LDLR.

#### MATERIALS AND METHODS

**cDNAs and Cells**—All NARC-1 and its mutants cDNAs were cloned in pIRES2-EGFP with a C-terminal V5 tag, as described (5). Antibody to LRP1 (C-terminal Ab377) was a generous gift of J. Herz (University of Texas, Dallas). Stable transfectants of empty bicistronic pIRES2-EGFP vector, V5-tagged wild type NARC-1 and its mutants H226A, S127R, and D374Y were obtained in the human hepatocyte-derived cell

line HepG2 following G418 selection and FACS purification of fluorescent cells (25).

**Transfections and Biosynthetic Analyses**—All transfections were done with  $3 \times 10^5$  HEK293 cells using Effectene (Qiagen) and a total of 1–1.5  $\mu\text{g}$  of cDNAs. Two days post-transfection, the cells were washed and then incubated for various times with either 250  $\mu\text{Ci/ml}$  [ $^{35}\text{S}$ ]Met/Cys or  $\text{Na}_2^{35}\text{SO}_4$  (PerkinElmer Life Sciences and Analytical Sciences) or 400  $\mu\text{Ci/ml}$  [ $^3\text{H}$ ]Ile (Amersham Biosciences). Pulse-chase experiments with [ $^{35}\text{S}$ ]Met/Cys, in the absence or presence of A23187 (2  $\mu\text{M}$ ), brefeldin A (2.5  $\mu\text{g/ml}$ ), thapsigargin (300 nM), or nocodazole (66 nM), were carried out as described previously (3, 26). The cells were lysed in modified RIPA buffer (150 mM NaCl, 50 mM Tris-HCl (pH 7.5), 1% Nonidet P-40, 0.5% sodium deoxycholate, and a protease inhibitor mixture (Roche Applied Science), after which the lysates and media were prepared for immunoprecipitations (26). The antibodies used were the monoclonal V5-mAb (1:500; Invitrogen) and LDLR-C7-mAb (1:200; Santa Cruz Biotechnology), and a rabbit antibody directed against amino acids 184–196 of human LDLR (1:400; Research Diagnostics Inc.). Immunoprecipitates were resolved by SDS-PAGE on 8% Tricine gels and autoradiographed. For Western blots, HepG2 cells were incubated in the presence or absence of 5 mM  $\text{NH}_4\text{Cl}$  overnight before cellular extraction in the above RIPA buffer lacking SDS. Most of these experiments were repeated at least three times. Quantitation was performed on a Storm Imager (Amersham Biosciences) by using the ImageQuant version 5.2 software.

**Subjects and FACS Analysis of Transformed Lymphoblasts**—Epstein-Barr virus (EBV)-transformed lymphoblasts (27) were obtained for subjects either heterozygote for the S127R mutation in the *PCSK9* gene or normolipidemic subjects (six of each) and a subject heterozygote for the P664L mutation in the *LDLR* gene. All subjects gave their informed consent. EBV-transformed lymphoblasts were cultured in Dulbecco's modified Eagle's medium (Invitrogen), 10% fetal calf serum (Biomedica), and 50 units/ml penicillin/streptomycin (Sigma). Lymphoblasts were stained with the LDLR-C7-mAb for 30 min on ice. Cells were then stained with a goat anti-mouse antibody conjugated to phycoerythrin (Santa Cruz Biotechnology) for 30 min on ice. Flow cytometry analysis was performed by using a FACScan Cytometer (BD Biosciences), and the data were analyzed using the CellQuest software package (BD Biosciences). For each sample, 10,000 live events were collected, and all results were confirmed by three independent experiments.

**Protein Solubilization, Western Blots, and LDLR and LRP1 Immunodetection**—Cells in 60-mm plates were incubated for 24 h in MEM plus either 10% fetal bovine serum with no addition or 10% lipoprotein-deficient serum plus 50  $\mu\text{M}$  compactin and 50  $\mu\text{M}$  mevalonate as in Ref. 28. The cells were washed, incubated for 10 min with 1.4% Triton X-100 buffer with protease inhibitors (Roche Applied Science) on ice, and homogenized, and the lysate was clarified (29). Fifty micrograms of proteins were analyzed by Western blot of LDLR (160 kDa) and LRP1 small subunit (85 kDa). The membranes were successively incubated with primary antibodies (1:400, LDLR; 1:3000, LRP1) and an appropriate secondary antibody and revealed using ECL Plus (Amersham Biosciences). Quantitation was performed as above.

**LDL Isolation and  $^{125}\text{I}$ -Protein Labeling**—Human normolipidemic plasma (Royal Victoria Hospital, Montreal, Quebec, Canada) was supplemented with 0.3 mM EDTA, 3 mM sodium azide, 10  $\mu\text{M}$  phenylmethylsulfonyl fluoride, and 10  $\mu\text{M}$  Trolox before the isolation of lipoproteins, which was achieved by ultracentrifugation as described (30). Human LDL ( $d = 1.025\text{--}1.063$  g/ml) were prepared as described (31). LDL and holotransferrin were  $^{125}\text{I}$ -labeled by a modification (32) of the iodine monochloride method. The specific radioactivity was  $\sim 1.5 \times 10^5$  cpm/ $\mu\text{g}$  of LDL or holotransferrin.

**$^{125}\text{I}$ -LDL Degradation Assay**—HepG2 cells in 6-well plates were incubated for 4 h at 37 °C with 10  $\mu\text{g}$  of  $^{125}\text{I}$ -LDL in a total volume of 500  $\mu\text{l}$  containing 250  $\mu\text{l}$  of MEM (2 $\times$ ) plus 4% BSA (MEM-BSA), pH 7.4, and the media were collected. The cells were washed once with 500  $\mu\text{l}$  of PBS plus 0.2% BSA and twice with 1 ml of PBS. Incubation media plus the first wash were pooled and precipitated with 12% trichloroacetic acid. Cells incubated with  $^{125}\text{I}$ -LDL were homogenized in 1.5 ml of 0.2 N NaOH, and the protein content was assayed (33). Degradation was estimated as  $\mu\text{g}$  of LDL protein/mg of cell protein.

**$^{125}\text{I}$ -Holotransferrin Recycling Assay**—To estimate the efficiency of iron-loaded holotransferrin (Sigma) recycling in HepG2 cells, cells in 12-well plates were incubated for 15 min at 37 °C with 0.5  $\mu\text{g}$  of  $^{125}\text{I}$ -transferrin in 250  $\mu\text{l}$  of MEM-BSA, pH 7.4 (pulse). Cell surface-bound  $^{125}\text{I}$ -transferrin was dissociated from the cells with three rapid washes with acetic saline (0.2 mM acetic acid and 500 mM NaCl, pH 2.5) on ice (34), followed by one wash with ice-cold PBS. Cells were re-fed with fresh MEM-BSA plus 50  $\mu\text{g/ml}$  unlabeled transferrin, and the cells

were incubated for 60 min at 37 °C (chase). Recycled <sup>125</sup>I-transferrin was the trichloroacetic acid-precipitable fraction, whereas cell-associated (bound plus internalized) <sup>125</sup>I-transferrin was measured by homogenizing the cells in 0.2 N NaOH. No degradation was detected during the chase phase.

**Microsequencing and Mass Spectrometry Analyses**—Transfected HEK293 cells were pulse-labeled with 400 μCi/ml [<sup>3</sup>H]Ile. Lysates were immunoprecipitated with the V5-mAb, resolved by SDS-PAGE (8% Tricine gel), and blotted on an Immobilon PSQ membrane (Millipore) and autoradiographed. The identified radioactive NARC-1 protein was microsequenced as described previously (26) on an Applied Biosystems Procise cLC Protein Sequencer. For cold sequencing, the secreted NARC-1 from the stable HepG2 transfectant was V5-immunoprecipitated, separated by SDS-PAGE (12% glycine gel), electroblotted onto polyvinylidene difluoride, and the purified band microsequenced.

For time-of-flight mass spectral analysis of immunocaptured V5-tagged NARC-1, 3 μl of 0.5 mg/ml protein A (in PBS, pH 8.2) was covalently bound to the spots of a pre-activated PS10 ProteinChip Array (CIPHERGEN Biosystems Inc., Palo Alto, CA) by incubation in a humid chamber at room temperature (RT) for 1 h. The protein A solution was removed, and residual pre-activated sites were blocked by incubation of the chip in 0.5 M ethanolamine in PBS (pH 8) for 15 min at room temperature. Following the blocking step, the chip was washed three times with PBS (pH 7.4) + 0.5% Triton X-100 for 15 min at room temperature. Cell lysates were prepared from stable HepG2 pools expressing V5-tagged NARC-1 or pIRES2-EGFP vector, grown in the absence or presence of 5 μg/ml tunicamycin for 18 h, and were preincubated with 1:1000 V5-mAb for 1 h at 4 °C and added to the spots containing protein A for 2 h at RT. Samples were removed, and the spots were sequentially washed at RT one time in PBS (pH 7.4) + 0.5% Triton X-100 for 15 min, three times in PBS (pH 7.4) for 15 min, and finally in 10 mM Hepes (pH 7.4) for 1 min. The chip was allowed to dry at RT, and 1 μl of saturated sinapinic acid (3,5-dimethoxy-4-hydroxycinnamic acid; Sigma) in 50% acetonitrile + 0.5% trifluoroacetic acid was added to each spot. Mass spectral analysis was performed by surface-enhanced laser desorption time-of-flight mass spectrometry (SELDI-TOF-MS) in a CIPHERGEN Protein Biology System II (PBS II). Analyses represent an average of 100 shots, and masses were calibrated externally with All-in-1 Protein Standards (CIPHERGEN Biosystems Inc., Palo Alto, CA).

**Ribonucleic Acid Interference Knockdown of NARC-1 mRNA in HepG2 Cells**—Three 19-mer double-stranded oligonucleotides were designed against different segments of human NARC-1 cDNA of the following sequences: 5'-AATGGTTCGACTTGTCTCCTC-3', 5'-AGCAAGTGTGACAGTCATGGC-3', and 5'-AGGCATTCAATCCTCAGGTCT-3'. These were cloned into pRNA-U6.1 vector (GenScript), and hygromycin-resistant pools of stable HepG2 transfectants were used to isolate individual clones. Their level of human NARC-1 mRNA was estimated by Northern blotting by using a cDNA probe, spanning nucleotides 484–1059, as described (5). Three selected clones, A, B, and C, were used to analyze the relative level of LDLR activity by fluorescent LDL uptake using FACS. The relative LDLR activity levels in the clones A–C were calculated with respect to the LDL uptake of control cells expressing the empty pRNA-U6.1 vector.

**In Vivo Expression of NARC-1 in Mice**—Wild type female and LDLR(–/–) C57BL/6 mice were obtained from The Jackson Laboratories (Bar Harbor, ME). Mice were maintained on a 12-h light/dark cycle and fed a chow diet. Before each study, serum cholesterol levels were determined, and the mice were divided into two groups such that the mean plasma cholesterol levels in the groups were not different. Each group contained four mice. Statistical analyses were performed by Student's *t* test. A value of *p* < 0.05 was considered significant.

Mice were injected intravenously via the tail vein with 1 × 10<sup>11</sup> particles of recombinant adenovirus on day 0 of the study. Blood was obtained from the retro-orbital plexus at various times before and after adenovirus injection. Mice were fasted 4 h before bleeding, and blood was always drawn at the same time of day. Aliquots of plasma were stored at –20 °C until analysis of lipids. Plasma cholesterol, HDL-C, and triglyceride levels were measured enzymatically on a Cobas Fara II (Roche Applied Science) using Sigma reagents. Non-HDL cholesterol levels were determined by subtracting HDL-C from the total cholesterol. Plasma samples (200 μl pooled from each group) were analyzed by FPLC (Amersham Biosciences) on Superose 6 columns in series as described previously (35). The cholesterol concentrations in the FPLC fractions were determined using an enzymatic assay (Wako Pure Chemical Industries Ltd., Osaka, Japan).

## RESULTS

**Mutations Affecting the Zymogen Processing of NARC-1**—We reported previously that the underlined residues in the prodomain sequence of proNARC-1, *i.e.* YVVVLKEETHL (where the underlined boldface L indicates the P1 cleavage position), play a critical role in the zymogen processing of pro-NARC-1 and concluded that Leu<sup>82</sup> ↓ may represent the zymogen-processing site. This was also based on the microsequencing results of secreted [<sup>3</sup>H]Leu NARC-1 that showed a Leu at position 6 (see the above sequence KEETHL). However, this deduction was not consistent with the observed apparent molecular mass of ~14 kDa on SDS-PAGE of the co-immunoprecipitating prosegment. It was indeed expected at ~6 kDa if the segment composed amino acids 31–82, starting from the signal peptide cleavage site (position 30 ↓ 31) to the presumed zymogen-processing site (position 82 ↓ 83) (5). Finally, N-terminal sequencing of NARC-1 by Edman's degradation was very inefficient and had to be repeated several times (5). Thus, we have decided to reinvestigate the exact processing site of pro-NARC-1 by two complementary approaches. First, we prepared large batches of human NARC-1 secreted from HEK293 or HepG2 cells. Sequencing of secreted cold NARC-1 identified the first three N-terminal residues as Ser-Ile-Pro, and microsequencing of the [<sup>3</sup>H]Ile-labeled protein revealed an Ile at position 2. These data would predict that the zymogen-processing site is rather SSVFAQ ↓ SIPWNL<sup>158</sup> (where Q indicates the P1 cleavage position). The presence of Leu<sup>158</sup> at the sixth position after the cleavage site would also be consistent with the current [<sup>3</sup>H]Ile data and our earlier [<sup>3</sup>H]Leu microsequencing results (5). Second, we analyzed by SELDI-TOF the exact mass of the immunoprecipitating NARC-1 and its ~14-kDa prosegment from HepG2 cells treated for 18 h with tunicamycin. As shown in Fig. 1A, *a*, the observed molecular masses of 58,800 ± 430 and 13,772 ± 100 Da closely agree with the calculated masses of V5-tagged nonglycosylated NARC-1 (58,695 Da for amino acids 153–692 + V5 tag) and the prosegment (13,772 Da for amino acids 31–152, N-terminal pyroglutamic acid (5) + 1 Met oxidation). As reported previously (5), Fig. 1A, *b*, shows that glycosylation of the single N-linked site of NARC-1 increases its molecular mass by 1727 to 60,527 Da, whereas the molecular mass of the nonglycosylated prosegment remains unchanged. We also observed heterogeneity in the molecular mass of the prosegment that may be partly explained by the presence of two Tyr-sulfation sites (see also Fig. 4B), resulting in a shoulder peak at ~13,995 Da (estimated as 13,993 Da for amino acids 31–152 + N-terminal pyroglutamic acid + 1 Met oxidation + Na<sup>+</sup> + K<sup>+</sup> + 2 Tyr-O-sulfation) (Fig. 1A, *a*). Therefore, we conclude that the autocatalytic zymogen processing of pro-NARC-1 occurs at SSVFAQ ↓ SIP. Based on this assignment, the S127R mutation (14) localizes within the prosegment of NARC-1, and the F216L (14) and D374Y (16, 17) mutations arise in the catalytic subunit (Fig. 1B). Three more natural *PCSK9* mutations were recently identified, namely R218S and R237W,<sup>2</sup> and the double Norwegian mutation D374Y + N157K (17).

The effect of mutations around the zymogen-processing site SSVFAQ ↓ SIP are shown in Fig. 2A. The data revealed that Val<sup>149</sup> and Pro<sup>155</sup> at the P4 and P3' positions of the cleavage site, respectively, are the most critical residues in this motif, because relative processing (RP) was reduced by >80%. However, the analysis of the triple mutation (S153G,I154T,P155S) representing the P' residues of the *Fugu rubripes* NARC-1 sequence revealed that Pro<sup>155</sup> can be replaced by Ser, indicating that the predicted β-turn following the cleavage site is critical. The hydrophobic Ile and Leu residues can replace the P4 Val, albeit resulting in lower efficacy of zymogen processing.

<sup>2</sup> C. Boileau and J. Davignon, personal communication.

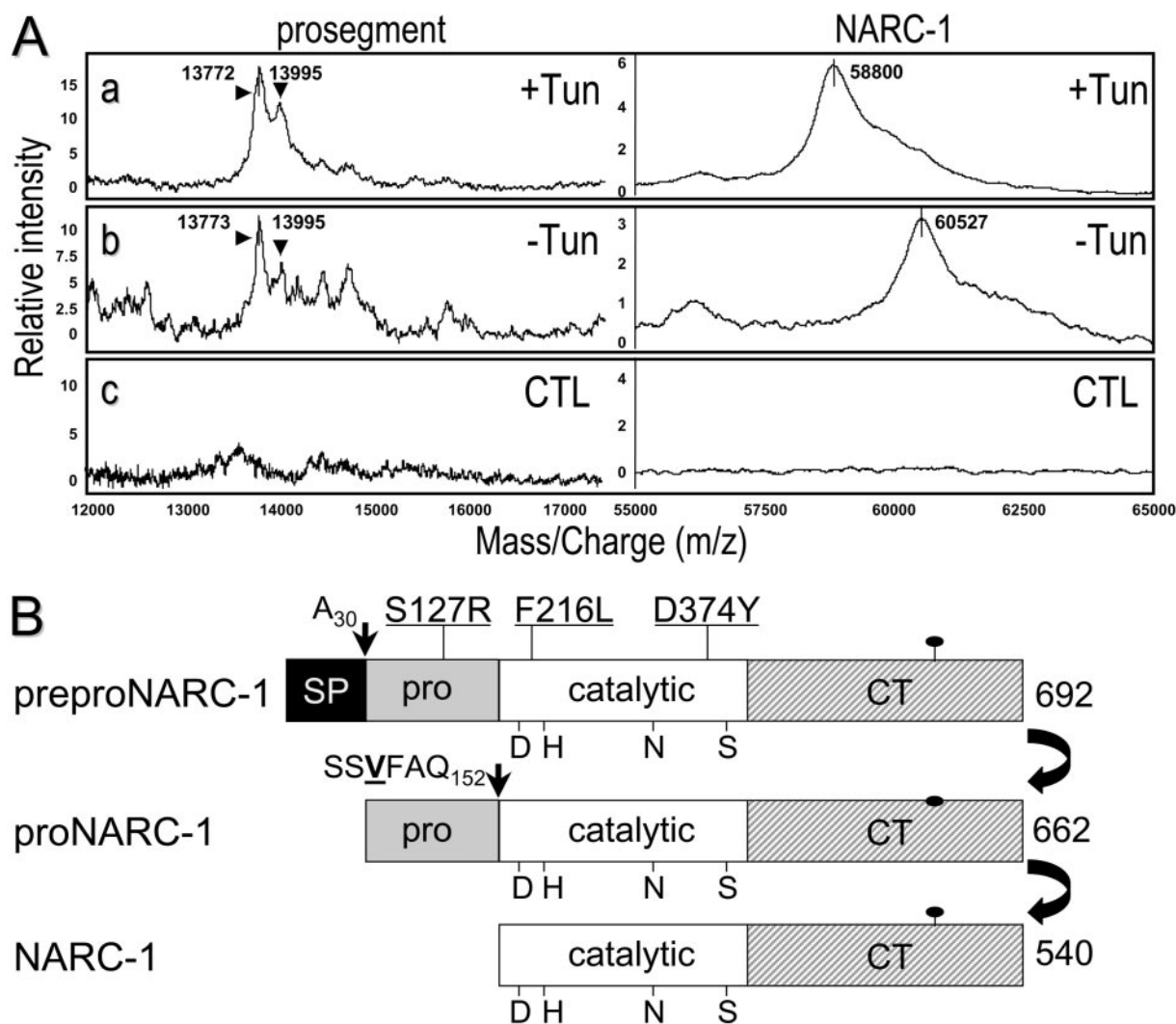


**FIG. 1. Mass spectral analysis of wild type and nonglycosylated NARC-1, their prosegments, and schematic representation of the processing of NARC-1.** *A*, *a–c* represent SELDI-TOF mass spectral analyses of the molecular masses of the proteins in the V5-immunoprecipitated cell lysates from HepG2 cells overexpressing either *N*-linked nonglycosylated V5-tagged NARC-1 (+*TUN*; grown in the presence of 5  $\mu$ g/ml tunicamycin for 18 h), V5-tagged NARC-1 (–*TUN*), or the control empty vector (*CTL*), respectively. *B* illustrates the positions of the genetic mutations S127R, F216L, and D374Y, as well as the signal peptide and zymogen-processing sites. The active sites Asp, His, Ser, and the oxyanion hole Asn as well as the sole *N*-glycosylation site are emphasized.

The enzyme tolerates Ala at P1 (RP  $\approx$ 0.8); Ser and Gly better than Leu (RP  $\approx$ 0.8) at P2; Ala poorly at P3 (RP  $\approx$ 0.4); Leu better than Phe (RP  $\approx$ 0.8) at P5; and Ala at P6.

In Fig. 2*B*, we compare the effects of natural and selected mutations, *e.g.* the active site H226A, and C-terminal truncations downstream of Gln<sup>454</sup> and Ser<sup>681</sup>. Whereas the S127R mutation resulted in  $\sim$ 50–60% decrease in zymogen processing, the mutants D374Y and H226A are not cleaved at all. In contrast, the double mutant D374Y + N157K did not result in very significant changes in the processing of pro-NARC-1 to NARC-1. The same holds true for the two natural French mutations F216L and R218S and the French Canadian R237W mutation. In attempting to evaluate the possible presence of a P-domain found in most of the other proprotein convertases and demonstrated to be critical for their folding and zymogen processing (36), except for SKI-1 (37), we also truncated the C terminus to end at Ser<sup>681</sup> ( $\perp$ S<sup>681</sup>) or Gln<sup>454</sup> ( $\perp$ Q<sup>454</sup>). Analysis of a similar truncation at an amino acid equivalent to Gln<sup>454</sup> was reported for rat NARC-1 (11). Neither truncations blocked zymogen processing and subsequent secretion, suggesting that NARC-1 does not possess a typical P-domain. However, we noticed that the  $\perp$ Q<sup>454</sup> truncation mutant is  $\sim$ 3-fold less well processed than the wild type zymogen. It is thus possible that the C-terminal Cys/His-rich domain

comprising amino acids 449–692 of NARC-1 (5) plays a role in zymogen folding/stabilization.

In view of the autocatalytic nature of the prosegment cleavage, the sequence surrounding the cleavage site is indicative of the enzymatic recognition motif of NARC-1. Therefore, we have embarked on a large mutagenesis study to assess the importance of the conserved and genetically mutated residues in the folding and/or processing of NARC-1 (Figs. 2 and 3). We can subdivide the mutants into three groups as follows: group 1 includes those that substantially ( $\geq$ 80%) block the zymogen processing of NARC-1; group 2 includes those that have milder effects; and group 3 encompasses silent mutations (Figs. 2 and 3). The group 1 single point mutations that drastically reduced NARC-1 processing and secretion are as follows: Y78A, V80A, V80L, L82A, L82P, M126A, P138Y, I143P, V149A; the Utah natural mutant D374Y; the active site mutant H226A; and the oxyanion hole mutant N317A (Figs. 2 and 3). The double mutant AA102RR and the triple mutants VVV79RRL and V79I/K83A/L112P also abrogated processing. Because the unprocessed zymogen does not exit the ER (5), this explains the lack of significant secretion in the above mutants. The group 2 mutations include the polymorphic variant containing two additional Leu (+LL) to the Leu stretch of the signal peptide (14),

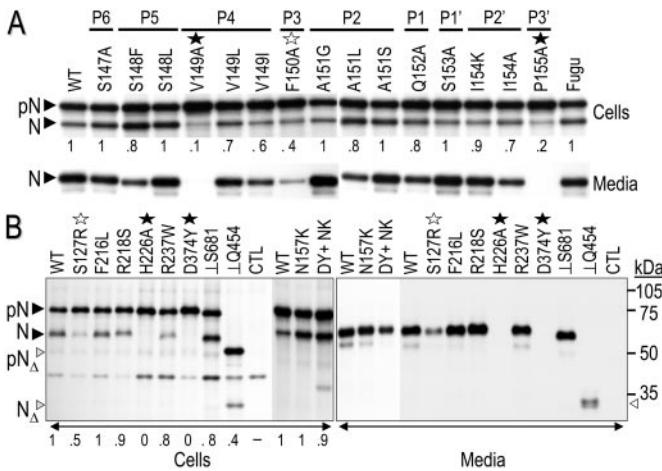


**FIG. 2. Specificity of the zymogen-processing site and effect of genetic mutations and deletions.** A and B, 40 h post-transfection, HEK293 cells expressing NARC-1 or its listed mutants were pulse-labeled with [<sup>35</sup>S]Met/Cys for 4 h and immunoprecipitated with the V5-mAb. Cell lysates and media were analyzed by SDS-PAGE on 8% Tricine gels. The *dark stars* emphasize the critical mutations, and the *open stars* indicate those that have a milder effect. B, the band migrating at ~40 kDa that appears sporadically is nonspecific, and it is also found in the control empty vector. Quantitations of the relative processing of NARC-1 (N) to pro-NARC-1 (pN), taking into account the levels in both cells and media (that of WT NARC-1 is taken as 1), are shown at the *bottom* of the cells panels.

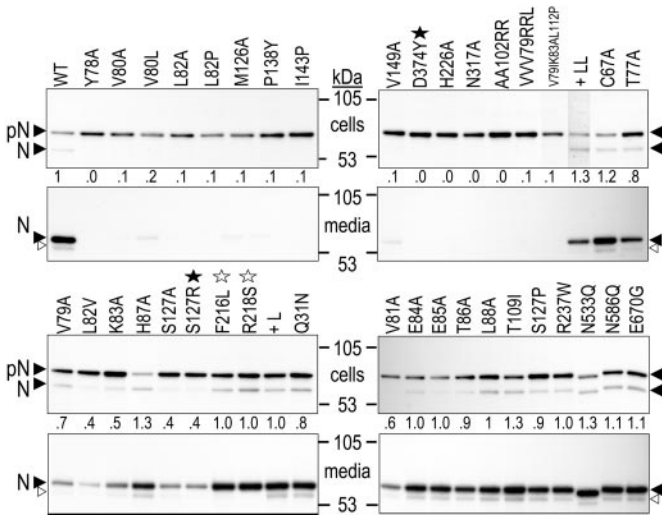


**FIG. 3. Biosynthetic analysis of wild type and NARC-1 mutants.** HEK293 cells were transiently transfected with a cDNA coding for V5-tagged NARC-1 or its represented mutants. Forty eight hours post-transfection, the cells were pulse-labeled with [<sup>35</sup>S]Met/Cys for 3 h. pN, pro-NARC-1; N, NARC-1.

T77A, V79A, V81A, L82V, K83A, S127A, and the French mutation S127R (see also Fig. 2B). In group 3 are included the three other natural mutations F216L, R218S, and R237W (see also Fig. 2B); the polymorphic variant containing one more Leu (+L) in the Leu stretch of the signal peptide (14); Q31N, C67A, and V80I (not shown); E84A, E85A, T86A, H87A, L88A, T109I, S127P, and N586Q; and the N-glycosylation N533Q, as well as the polymorphic E670G mutations (14). Thus, multiple mutations in the unprocessed protein either before or after the processing site seem to disturb the conformation of the protein and affect its autocatalytic processing. Among the most dramatic mutations are those previously reported within the internal  $\beta$ -strand motif **YXVXL**<sup>S2</sup> (5) of the prosegment, as well as the amino acid preceding Ser<sup>127</sup>, *i.e.* M126A, and the mutant found in the Utah pedigree D374Y (16). Notably, the level of the

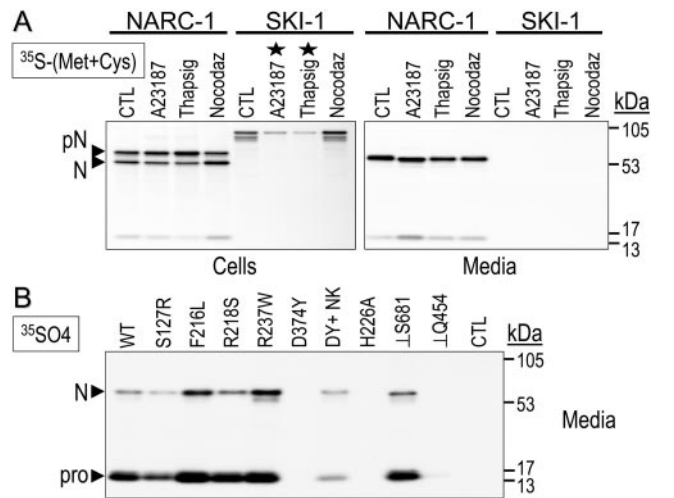


**FIG. 4. Ca<sup>2+</sup> dependence and sulfation of NARC-1.** HEK293 cells were transiently transfected with cDNAs encoding either V5-tagged human NARC-1 or its mutants or SKI-1. Forty hours post-transfection, the cells were pulse-labeled for 4 h with [<sup>35</sup>S]Met/Cys (A) or 2 h with Na<sub>2</sub>[<sup>35</sup>SO<sub>4</sub>] (B) in the absence or presence of A23187, thapsigargin, or nocodazole. The cell lysate and media were then immunoprecipitated with a V5-mAb, and the immunoprecipitates were separated by SDS-PAGE on an 8% Tricine gel and autoradiographed. The migration positions of pro-NARC-1 (pN), NARC-1 (N), and its ~14-kDa prosegment (*pro*) are emphasized. A, the *stars* point out the inhibition of zymogen processing of SKI-1 by A23187 and thapsigargin.

minor form of secreted NARC-1 seems to be quite reduced in the R218S and F216L natural mutants (Figs. 2B and 3). Whether this is an N-terminal autolysis fragment awaits further analysis.

**Calcium Independence and Sulfation of NARC-1**—To test whether the autocatalytic processing of pro-NARC-1 to NARC-1 requires Ca<sup>2+</sup>, as for all the other convertases (1, 3), we expressed in HEK293 cells either human SKI-1 or NARC-1 tagged with a C-terminal V5 epitope, and we analyzed the fate of the *de novo* biosynthesized proteins following pulse-labeling of the cells with [<sup>35</sup>S]Met/Cys for 4 h (Fig. 4A). As reported previously, proSKI-1 (~105 kDa) is converted to the B/B' and C forms of SKI-1 that remain attached to the membrane (3, 37), whereas proNARC-1 is processed to NARC-1 and is secreted as a complex with its ~14-kDa prosegment (5) (Fig. 4A). However, if the cells are preincubated with the Ca<sup>2+</sup> ionophore A23187 (38) or the Ca<sup>2+</sup>-ATPase inhibitor thapsigargin (39), zymogen processing of proSKI-1 is blocked, whereas that of pro-NARC-1 goes on unabated. This demonstrates that different from SKI-1, autocatalytic conversion of pro-NARC-1 to NARC-1 within the endoplasmic reticulum (ER) is not dependent on Ca<sup>2+</sup>. However, we did notice that the secreted NARC-1 migrates with a lower apparent molecular mass when the cells were incubated with A23187 (Fig. 1), suggesting that Ca<sup>2+</sup> affects a post-translational modification(s) of NARC-1. In contrast, the microtubule inhibitor nocodazole, which causes the disassembly of microtubules and disorganization of the Golgi complex (40), does not affect the zymogen processing of either convertase (Fig. 4A), in agreement with the ER-localized zymogen processing events.

Inspection of the primary sequence of NARC-1 revealed two possible Tyr-sulfation motifs (41) within its prosegment at Tyr<sup>38</sup> and Tyr<sup>142</sup>. Most interestingly, whereas Tyr<sup>38</sup> is only present in mammalian NARC-1, Tyr<sup>142</sup> is also conserved in fish (*F. rubripes* and *Zebrafish*) NARC-1. Pulse-labeling of HEK293 cells transiently overexpressing NARC-1 with Na<sub>2</sub>[<sup>35</sup>SO<sub>4</sub>] revealed that secreted NARC-1 and its prosegment are sulfated (Fig. 4B) and did not significantly accumulate in cells (not shown). This agrees with the fact that sulfation is a late post-

translational modification occurring in the *trans*-Golgi network (42). We also found that the level of sulfation of the prosegment (~14 kDa) is higher than that of the mature NARC-1 (compare their ratio in Fig. 4, A and B), suggesting that both Tyr<sup>38</sup> and Tyr<sup>142</sup> are sulfated and that another sulfation site exists in mature NARC-1, possibly on the single sugar moiety because no Tyr-sulfation motif is found in the primary sequence of the mature enzyme. The absence of sulfation of the H226A and D374Y mutants is in accord with their major localization in the ER (endoH-sensitive forms, not shown).

**The S127R Mutation Reduces the Level of LDLR in the Lymphocytes of Patients**—Mutations in the NARC-1 gene *PCSK9* are associated with the development of familial hypercholesterolemia (14, 16), and recent kinetic studies in the S127R patients revealed an increased hepatic apoB100 production and mildly reduced LDL clearance (43). We thus tested if the level of LDLR was affected in hypercholesterolemic subjects carrying the S127R mutation. For this purpose, we estimated the level of LDLR at the surface of lymphoblasts from normal and affected subjects by FACS, and we compared them to the LDLR levels of patients with a P664L mutation in the *LDLR* gene. The latter mutation affects the post-translational modifications of the LDLR impairing its transport between the ER and the Golgi apparatus (44). As expected, FACS analysis on the lymphoblasts of the subjects carrying the LDLR mutation P664L revealed that they express ~42% less LDLR at the cell surface *versus* normal subjects ( $2.2 \pm 0.2$  *versus*  $3.8 \pm 0.9$ ,  $p = 0.01$ ) (Fig. 5, *top two panels*). Similar results were obtained for the lymphoblasts of two subjects carrying the S127R mutation in the *PCSK9* gene (Fig. 5). The mean level of the cell surface LDLR was reduced on average by ~35% as compared with normal subjects ( $2.5 \pm 0.8$  *versus*  $3.8 \pm 0.9$ ,  $p = 0.02$  for the HC2 family; and  $2.4 \pm 1.1$  *versus*  $3.8 \pm 0.9$ ,  $p = 0.04$  for the HC92 family). These observations indicate that, as in FH heterozygotes (*LDLR* mutation carriers), S127R mutation carriers express less LDLR at the cell surface than normocholesterolemic subjects.

**Overexpression of NARC-1 and Its S127R Mutant Reduces the Level of LDLR in HepG2 Cells**—We obtained stable HepG2 pools overexpressing wild type (WT) NARC-1, and its S127R and active site H226A mutants (Fig. 6, A and C). We consistently observed that the level of expression of the WT enzyme is much below that of the other transfectants (Fig. 6A). Western blot analyses revealed that LDLR is significantly reduced in two independent pools overexpressing the mutant S127R (S127R-1 and S127R-2) but not in the H226A pool or the low expressing WT one (Fig. 6B, *upper panel*). Similar conclusions were reached upon measurement of the degradation of <sup>125</sup>I-LDL (Fig. 6B, *lower panel*). The observed reduction of the LDLR is specific, because no effect was observed on the protein levels of the related protein LRP1 (Fig. 6D, *upper panel*). Finally, the expression of S127R does not affect the general internalization machinery of the cells, as evidenced by the normal recycling of <sup>125</sup>I-transferrin (Fig. 6D, *lower panel*). However, cells enriched in NARC-1 by FACS sorting for EGFP expression (WT(+)) showed a significant reduction in LDLR levels (Fig. 6C).

We next tested whether any of the above HepG2 stable NARC-1 transfectants result in a modified LDLR processing and/or cellular trafficking. Pulse-chase analysis of the endogenous LDLR in HepG2 cells demonstrated that, within the studied time period, NARC-1 and its mutants do not cleave the LDLR, nor do they affect its exit rate from the ER (Fig. 7A). This suggested that the loss of LDLR in the S127R mutant does not occur in the ER or Golgi and is likely a late event, possibly related to the kinetics of its endocytosis and/or endosomal/

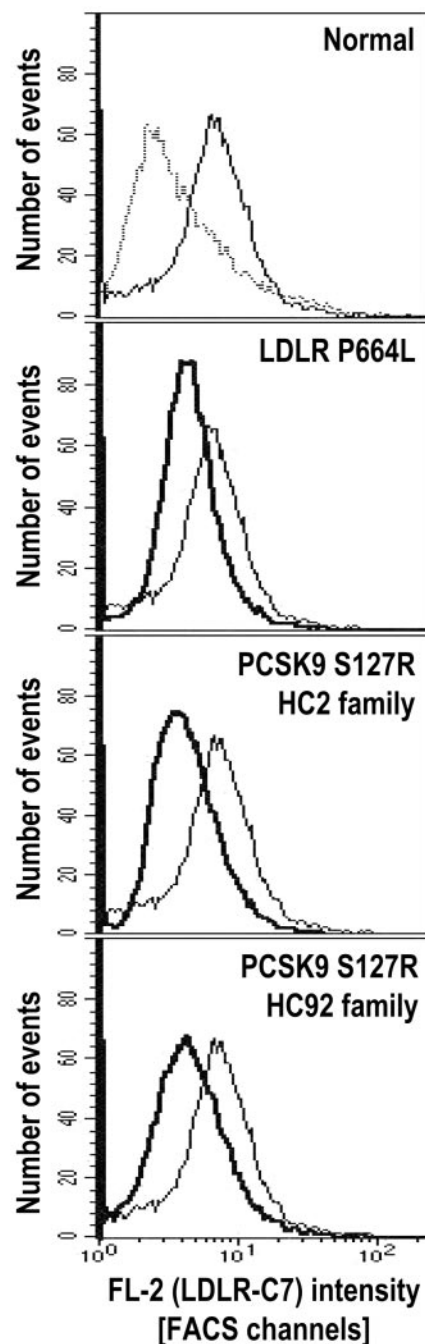


**FIG. 5. FACS analysis of LDLR expression in EBV-transformed lymphoblasts from a normal subject, *LDLR*, and *PCSK9* mutations carriers.** EBV-transformed lymphoblasts were incubated with the mAb LDLR-C7, washed in PBS, and stained with a phycoerythrin-conjugated secondary antibody. The *dotted line* corresponds to a sample stained with the secondary antibody only. The *solid lines* correspond to cells from a normal subject, and the *boldface lines* correspond to cells from hypercholesterolemic subjects (subject III-10 from HC2 family (see Fig. 1 in Ref. 62) and subject IV-3 from HC92 family (see Fig. 1 in Ref. 14)).

lysosomal degradation. To test this hypothesis, we incubated the S127R overexpressing HepG2 cells with the lysosomotropic  $\text{NH}_4\text{Cl}$ , an agent known to result in the alkalization of the pH of acidic compartments including those of the Golgi and endosomes/lysosomes (24, 45). The data revealed that although 5 mM  $\text{NH}_4\text{Cl}$  leads to ~1.5-fold increased levels of LDLR in control HepG2 cells expressing the vector alone, it rescues the loss of LDLR levels in those expressing the S127R mutant (~3.5-fold increase), without affecting the zymogen processing

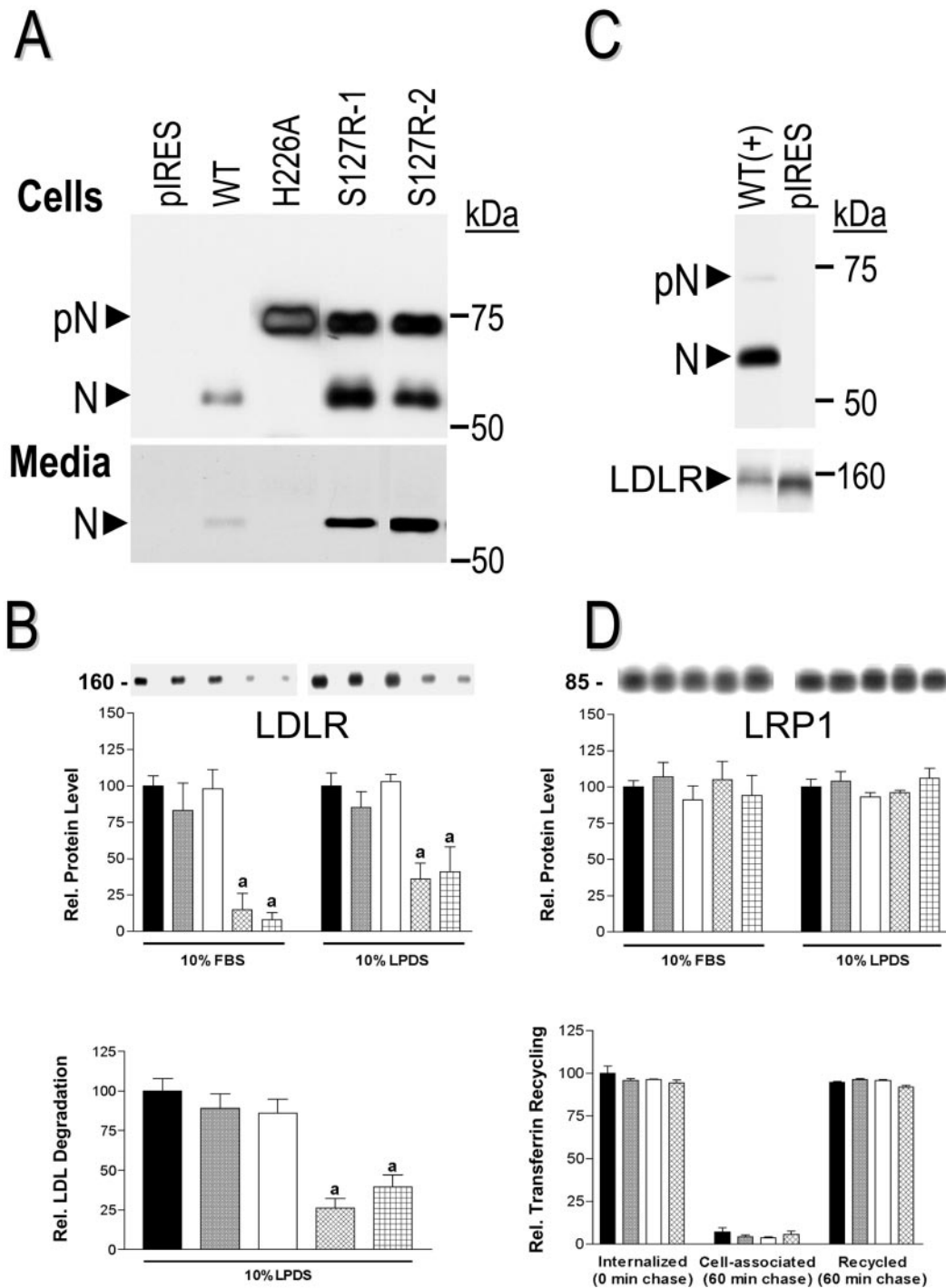


FIG. 6. **Assessment of the LDLR expression and activity in HepG2 cell lines.** A and C, Western blot of cell lysates and media of stable transfectants in HepG2 cells of NARC-1-V5, its active site mutant H226A, the natural mutants S127R (pools 1 and 2), and the enriched WT NARC-1 pool (WT (+)). Empty vector, *black bars*; WT NARC-1, *shaded bars*; H226A, *open bars*; and S127R (two pools), *cross-hatched bars*. Western blot analysis ( $n = 5$ ) of B, upper, and C, LDLR; and D, upper, LRP1. B, lower, measurement of LDLR activity ( $^{125}\text{I}$ -LDL degradation). The mean value for plasmid with an internal ribosomal entry site control cells was  $260 \pm 33 \mu\text{g}$  of protein/mg of cell protein ( $n = 6$ ). D, lower, assessment of  $^{125}\text{I}$ -holotransferrin recycling ( $n = 3$ ). pIRES values were set at 100%.

of NARC-1 (Fig. 7B). This suggests that the overexpressed S127R mutant somehow increases the metabolic rate of the LDLR. This may be because of the high level of expression of the S127R protein/enzyme or to a dominant effect of the mutation itself.

**Effect of NARC-1 Silencing on LDLR Activity**—HepG2 clones stably expressing one of three double-stranded oligonucleotides designed against different segments of human NARC-1 cDNA (A–C) were analyzed by Northern blotting.

The best silencing of NARC-1 mRNA was observed in A and C. FACS measurements of fluorescent LDL uptake revealed the highest amount of internalized LDL in A (~2.1-fold), whereas B and C exhibited intermediate levels (Fig. 8). This suggests that NARC-1 is involved in the maintenance of appropriate levels of LDLR and that its loss results in up-regulation of the receptor.

**Adenoviral Expression of Human Wild Type NARC-1 in Mice**—The effects of expression of human WT NARC-1 on

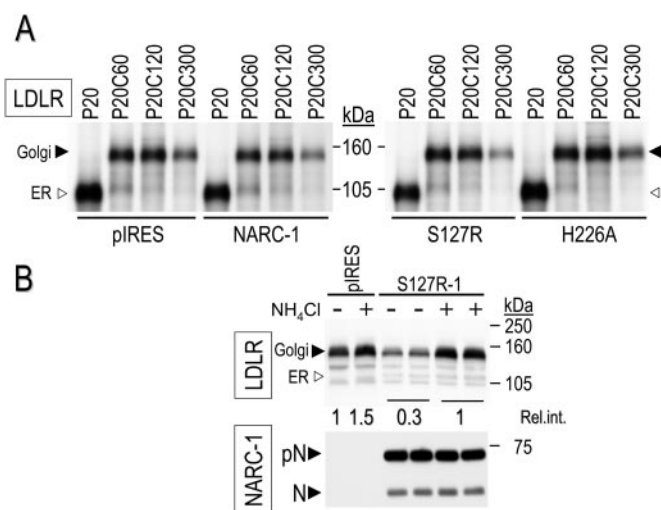


**FIG. 7. Analysis of the LDLR trafficking in HepG2 cells stably expressing NARC-1 and its mutants.** A, biosynthetic analysis of the LDLR. The open arrow points to the endoH-sensitive (not shown) ER-form of the LDLR at the 20-min pulse period (P20) and its transformation into the Golgi endoH-resistant form (dark arrow) at the chase periods 60 (P20C60), 120 (P20C120), and 300 (P20C300) min. B, effect of 5 mM NH<sub>4</sub>Cl on the level of endogenous LDLR in the S127R-1 stable pool as compared with that of the control cells expressing the vector alone (pIRES). pIRES, mammalian expression vector.

plasma lipids in either C56BL/6 wild type or LDLR(−/−) mice are shown in Fig. 9. Wild type mice injected with control vector (Ad-null) had no changes in their plasma lipids over the course of the study. In contrast, as observed from day 3 post-infection, expression of human NARC-1 resulted in a dramatic increase of non-HDL cholesterol (Fig. 9A) and total cholesterol (not shown) levels. However, minimal changes in triglyceride levels were observed (not shown). On day 7, Western blot analysis of the liver lysates of these mice using the V5-mAb clearly showed the presence of both pro-NARC-1 and NARC-1 (Fig. 9B, inset). Analysis of the lipoprotein distribution by FPLC on day 7 after virus injection confirmed a major elevation in LDL-C levels, but little change in very low density lipoprotein levels, in human NARC-1-expressing mice (Fig. 9B). The peak of change of non-HDL cholesterol was up by ~9-fold at day 7, which is consistent with the peak expression of protein using adenovirus as a gene transfer tool *in vivo* (46). The cholesterol peak of the LDL fraction coincides with the maximal apoB protein detected by Western blotting (not shown). Therefore, overexpression of human NARC-1 in mice resulted in accumulation of LDL particles *in vivo*. Because pulse-chase analysis in the LDLR negative cell line CHO-Id1A-7 (47) revealed normal NARC-1 zymogen processing (not shown), we also evaluated the effect of NARC-1 overexpression in LDLR(−/−) mice. Most surprisingly, this resulted in a delay in the time at which the up-regulation in LDL-C appears, *i.e.* instead of day 3 in normal mice, an ~84% increase was detected at day 7 (Fig. 9C). Analysis of the lipoproteins by FPLC indicated substantial increases in both very low density lipoproteins and LDL. This suggests that the time at which the increase in circulating LDL-C is observed is partially dependent on LDLR and that NARC-1 may also up-regulate apoB production in an LDLR-independent fashion.

#### DISCUSSION

The discovery of NARC-1 as the ninth member of the proprotein convertase family (5, 11), its high expression in liver and small intestine (5), and the identification of hypercholesterolemic patients carrying mutations in its gene (14, 16, 17), in addition to other recently published data (19–21), indicate a

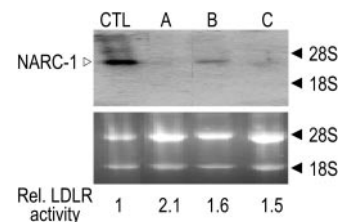


**FIG. 8. Knockdown of NARC-1 mRNA in HepG2 cells and its effect on LDLR activity.** Northern blot analysis of NARC-1 mRNA levels in HepG2 cells stably expressing three different ribonucleic acid interference (lanes A–C) or an empty vector (pRNAU6.1; pRNA). Three hygromycin-resistant clones A–C were isolated, and their RNA was hybridized with a <sup>32</sup>P-radiolabeled NARC-1 probe. The migration positions and the levels of the 18 S and 28 S ribosomal RNAs on the same blot are shown for comparison. At the bottom is listed the calculated relative activity of the LDLR with respect to the control (CTL) cells transfected with the empty vector, as estimated by FACS analysis of fluorescent LDL uptake (average of two experiments).

fundamental role of this enzyme in cholesterol metabolism. Nothing is known about the physiological substrates of NARC-1, nor whether it functions intracellularly and/or extracellularly. One approach to tackle this problem was to first define its enzymatic cleavage specificity and characteristics. Here, we demonstrate that the zymogen processing of NARC-1 does not depend on Ca<sup>2+</sup>, which sets NARC-1 apart from SKI-1 (Fig. 4) and all the other proprotein convertases. Microsequencing and mass spectrometric analyses of human NARC-1 and its associated prosegment (Fig. 1) revealed that the exact processing site occurs at the motif SSVFAQ<sub>152</sub> ↓ SIP (Fig. 1). This agrees with the site recently reported for rat NARC-1 (11). Site-directed mutagenesis suggested that P4 Val<sup>149</sup> and P3' Pro<sup>155</sup> are the most critical amino acids in this motif, with lesser contributions by P3 Phe<sup>150</sup> (Fig. 2A). However, the P' residues Ser-Ile-Pro<sup>155</sup> of human NARC-1 can be replaced by the *F. rubripes* Gly-Thr-Ser<sup>155</sup> sequence (Fig. 2A). Thus, we believe that secondary structures, such as the predicted β-turn imposed by either sequence, may influence the cleavage specificity, and hence caution should be applied regarding the exact motif recognized by NARC-1. By using various substrates, the *in vitro* activity of secreted human NARC-1 in the medium has consistently been very low in our hands (5). We attributed this low activity to the presence of stoichiometric amounts of the presumably inhibitory prosegment in complex with NARC-1 (see Fig. 4). A recent study (11) suggested that deletion of ~230 C-terminal amino acids of rat NARC-1 greatly enhances the measured activity *in vitro*. Thus, the absence of a typical P-domain (Fig. 2), coupled to the *ex vivo* (Fig. 4) and *in vitro* (11) Ca<sup>2+</sup>-independent activity of NARC-1, really sets this enzyme apart from the other convertases, because all the other members require a P-domain (equivalent to amino acids 474–573) for folding and Ca<sup>2+</sup> for activity (48–50). Finally, although NARC-1 is Tyr-sulfated in its prosegment and its carbohydrate moiety, PC1, PC2, and PC5 are Tyr-sulfated in their catalytic and/or C-terminal domains (51, 52). The functional importance of the Tyr-sulfation of the convertases is not known.

A large percentage of genetic diseases linked to amino acid substitutions or deletions result from misfolded proteins (53). Compared with wild type, missense mutant proteins are generally synthesized in a normal fashion but can be impaired in their folding and/or cellular trafficking. All the convertases known to date possess an N-terminal prosegment that acts both as an intramolecular chaperone and as a potent inhibitor of the enzyme. In addition, autocatalytic cleavage of the prosegment, at one or two sites, is a prerequisite to enzymatic activity (1, 6). Our work aimed to define whether the NARC-1 natural mutations affect the autocatalytic processing of pro-

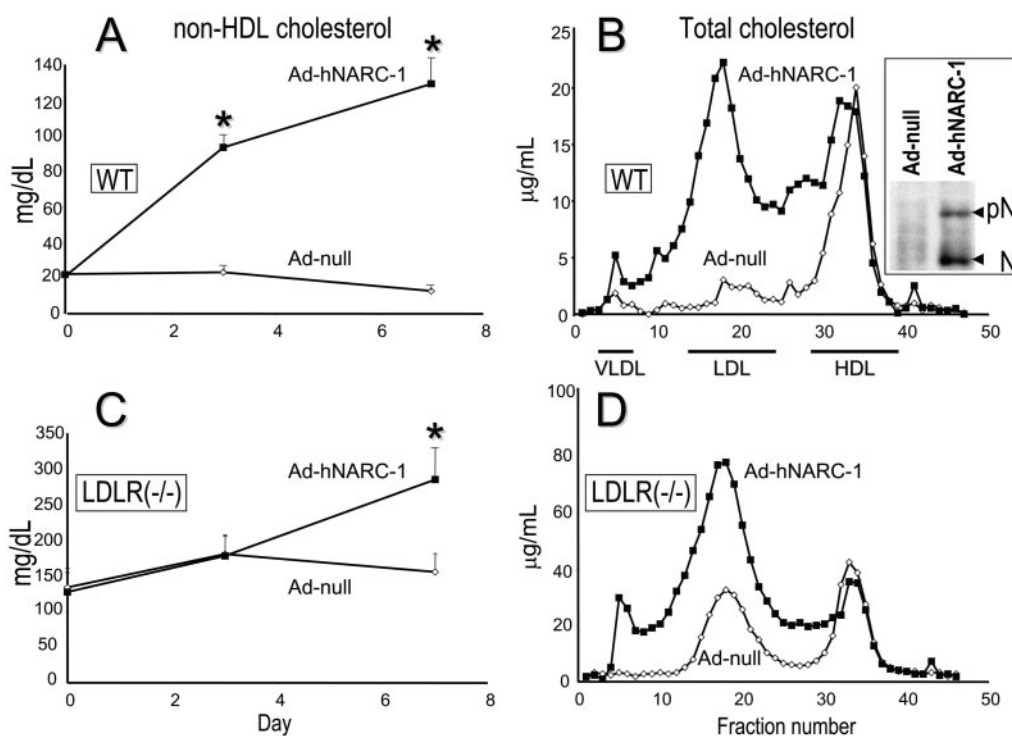


FIG. 9. Adenoviral expression of human NARC-1 in mice. Time course analysis of non-HDL cholesterol levels in wild type (A) and LDLR(-/-) mice (C) injected with Ad-hNARC-1 (squares) and Ad-null (diamonds) over the course of the study. Representative FPLC profile of wild type (B) and LDLR(-/-) mice (D) 7 days after injection of Ad-hNARC-1 (squares) and Ad-null (diamonds). B, inset represents a Western blot analysis using the V5-mAb of mice liver lysates obtained at 7 days post-infection with either wild type (Ad-null) or recombinant human NARC-1 (Ad-hNARC-1) adenovirus. Data are presented as mean  $\pm$  S.E. \* indicates significant ( $p < 0.05$ ) differences from the Ad-null group.

NARC-1 into NARC-1 (Figs. 2–4). Extensive mutagenesis data revealed that in HEK293 and HepG2 cells, of the six mutants known, only the S127R and especially D374Y variants exhibited a significant slowdown of the zymogen processing of NARC-1 by  $\sim 50$  and  $\sim 98\%$ , respectively. Molecular modeling indicates that Asp<sup>374</sup>, a highly conserved residue among the PC family members (54), is close to the active site pocket and stabilizes it, whereas Tyr<sup>374</sup> would not (not shown). Amazingly, the neutral N157K mutation, located at the P4' position of the autocatalytic site, reverted the effect of the D374Y mutation on zymogen processing (Figs. 2B and 4B). It is not yet known if the hypercholesterolemic Norwegian patient exhibiting the double heterozygote mutation (17) carries both mutations on the same allele.<sup>3</sup> Should the disease be related to the loss of NARC-1 activity, our data suggest that each mutation would be on a different allele.

We propose that at least for the D374Y and the S127R mutants, the major slowdown of pro-NARC-1 processing contributes to the pathology. However, the apparent normal processing of F216L, R218S, and R237W mutants suggests that multiple mechanisms lead to hypercholesterolemia, as reported for the LDLR (15, 55). In addition, it is not yet clear whether the NARC-1 dominant mutations lead to a loss or gain of function. Loss of function mutations may affect NARC-1 activity, its ability to bind substrates, or its cellular trafficking. On the other hand, gain of function mutations may be related to novel properties of NARC-1, such as zymogen binding to ER partners, cleavage of cryptic substrate(s) due to mislocalization, or modified enzymic specificity. In that context, a mutation in superoxide dismutase 1 (SOD1) that did not affect the expression or activity of the enzyme, caused a new protein-protein interaction with an aminoacyl tRNA synthetase, which resulted in mistargeting of the enzyme and thus amyotrophic

lateral sclerosis (56). Once a physiological substrate of NARC-1 is identified, it will be informative to assess whether *in cis* zymogen processing truly reflects the *in trans* activity of the enzyme on another substrate than itself.

A recent study investigated the *in vivo* kinetics of apoB100-containing lipoproteins in subjects carrying the S127R mutation (43). They exhibited a higher production rate of apoB100 ( $\sim 3$ -fold *versus* controls and  $\sim 1.5$ -fold *versus* LDLR-mutated patients). LDL fractional catabolic rate was also slightly decreased compared with controls ( $\sim 30\%$ ) but remained higher compared with that of LDLR-mutated patients ( $\sim 2$ -fold). FACS analysis revealed that the lymphoblasts of these S127R patients exhibit  $\sim 35\%$  lower levels of cell surface LDLR (Fig. 5). In agreement, in HepG2 cells stably expressing the S127R mutant,  $\sim 75\%$  lower levels of LDLR were detected (Fig. 6B). Most interestingly, this reduction seems to be abrogated if the cells are incubated with the lysosomotropic agent NH<sub>4</sub>Cl (24), which increases the pH of acidic compartments (Fig. 7B). This suggests that although NARC-1 does not seem to cleave the LDLR (Fig. 7A) or its transcriptional regulator SREBP2 (not shown), overexpression of the protease somehow down-regulates the LDLR cell surface levels, likely through enhanced endosomal/lysosomal degradation. How this endosomal/lysosomal pathway is regulated by NARC-1 and how it differs from the one regulated by the molecular adapter protein ARH (57) have yet to be defined.

The proportion of apoB that escapes post-translational degradation within the secretory pathway determines the production rate of apoB-containing lipoproteins. Twisk *et al.* (58) showed that the interaction of apoB with the LDLR within the secretory pathway is associated with increased apoB degradation and reduced apoB secretion. Thus, when intracellular LDLR is low, apoB appears *in vitro* (58) and *in vivo* (59) to be secreted in higher quantities. Preliminary results suggest that apoB is not a NARC-1 substrate (not shown). The enzyme may

<sup>3</sup> T. Leren, personal communication.

act through a change in the cellular environment of the receptor and/or the rate of lipidation of apoB by the microsomal triglyceride transfer protein complex, needed for the assembly and secretion of chylomicrons and very low density lipoproteins (60). This would account for the high hepatic secretion rate of apoB-containing lipoproteins in the S127R patients (43).

Indeed, adenoviral expression of wild type human NARC-1 in mice resulted in a gradual increase in the levels of circulating LDL cholesterol and apoB, peaking at ~9-fold at day 7 after infection, with no significant effect on plasma triglycerides (Fig. 9). While this manuscript was in preparation, similar results were reported with adenoviral overexpression of mouse NARC-1 in mice (61), indicating similar *in vivo* effects of overexpressed human and mouse NARC-1. The available data suggest that NARC-1 is implicated in both increased hepatic apoB production and reduced clearance of LDL. In agreement, overexpression of NARC-1 in LDLR(-/-) mice also resulted in a further increase in LDL cholesterol (~2-fold at day 7; Fig. 9C), indicating that the *in vivo* effects of overexpressed NARC-1 on the levels of circulating LDL cholesterol are not exclusively dependent on the LDLR. In their study on LDLR(-/-) mice, Maxwell and Breslow (61) did not observe such an elevation in LDL cholesterol, possibly because they analyzed this parameter up to day 4 following infection. We also obtained evidence that overexpression of human NARC-1 and its S127R mutant, but not its inactive H226A mutant, resulted in a similar loss of LDLR in HepG2 cells (Fig. 6). Because the inactive site mutant H226A had no effect, the observed effect upon overexpression could be enzymatic in nature. How then can we explain the negative effect of NARC-1 and its mutants on the level of cell surface LDLR? Could it be that a molecule pro-X stabilizes the receptor at the cell surface and that high levels of NARC-1 override this effect, possibly via processing of pro-X into X, which would then result in a rapid internalization and degradation of the LDLR? On the other hand, could NARC-1 mutants also diminish the level of cell surface LDLR through a different mechanism, via a dominant negative effect preventing LDLR stabilization or slowing down the rate of transit of the pro-X-LDLR complex to the cell surface? A direct consequence of this model is that, in the absence of NARC-1, the level of the LDLR is expected to increase. Indeed, in HepG2 cells stably expressing short interfering RNAs against NARC-1, the relative LDLR activity increased ~2.1-fold (Fig. 8).

In conclusion, although the abundance of NARC-1 in liver and intestine is in agreement with its cholesterologenic role, the differential zymogen processing observed between the NARC-1 natural mutants implies heterogeneous mechanisms behind PCSK9-related ADH. Furthermore, it remains to be elucidated whether the protease that is also present in developing neural tissues and kidney (5) fulfills functions unrelated to cholesterol metabolism via the cleavage of distinct substrates.

**Acknowledgments**—We thank M. Krieger for the generous gift of CHO-IIdA-7 cells and J. Herz for the LRP1 antibody. We also thank Brian Wilkes for the tridimensional modeling of NARC-1, Gaetan Mayer for critically reading the manuscript, and Andrew Chen for the microsequencing of NARC-1. The secretarial assistance of Brigitte Mary was greatly appreciated. We thank Marie-Christine Wagner (Plateforme de Cytométrie, Institut Pasteur, Paris, France) for excellent assistance and helpful discussions in FACS analyses.

#### REFERENCES

- Seidah, N. G., and Chretien, M. (1999) *Brain Res.* **848**, 45–62
- Zhou, A., Webb, G., Zhu, X., and Steiner, D. F. (1999) *J. Biol. Chem.* **274**, 20745–20748
- Seidah, N. G., Mowla, S. J., Hamelin, J., Mamarbachi, A. M., Benjannet, S., Toure, B. B., Basak, A., Munzer, J. S., Marcinkiewicz, J., Zhong, M., Barale, J. C., Lazure, C., Murphy, R. A., Chretien, M., and Marcinkiewicz, M. (1999) *Proc. Natl. Acad. Sci. U. S. A.* **96**, 1321–1326
- Sakai, J., Rawson, R. B., Espenshade, P. J., Cheng, D., Seegmiller, A. C., Goldstein, J. L., and Brown, M. S. (1998) *Mol. Cell* **2**, 505–514
- Seidah, N. G., Benjannet, S., Wickham, L., Marcinkiewicz, J., Jasmin, S. B., Stifani, S., Basak, A., Prat, A., and Chretien, M. (2003) *Proc. Natl. Acad. Sci. U. S. A.* **100**, 928–933
- Seidah, N. G., and Prat, A. (2002) *Essays Biochem.* **38**, 79–94
- Thomas, G. (2002) *Nat. Rev. Mol. Cell. Biol.* **3**, 753–766
- Taylor, N. A., Van de Ven, W. J., and Creemers, J. W. (2003) *FASEB J.* **17**, 1215–1227
- Roebroek, A. J., Umans, L., Pauli, I. G., Robertson, E. J., van Leuven, F., Van de Ven, W. J., and Constam, D. B. (1998) *Development (Camb.)* **125**, 4863–4876
- Yang, J., Goldstein, J. L., Hammer, R. E., Moon, Y. A., Brown, M. S., and Horton, J. D. (2001) *Proc. Natl. Acad. Sci. U. S. A.* **98**, 13607–13612
- Naureckiene, S., Ma, L., Sreekumar, K., Purandare, U., Lo, C. F., Huang, Y., Chiang, L. W., Grenier, J. M., Ozenberger, B. A., Jacobsen, J. S., Kennedy, J. D., DiStefano, P. S., Wood, A., and Bingham, B. (2003) *Arch. Biochem. Biophys.* **420**, 55–67
- Jackson, R. S., Creemers, J. W., Ohagi, S., Raffin-Sanson, M. L., Sanders, L., Montague, C. T., Hutton, J. C., and O'Rahilly, S. (1997) *Nat. Genet.* **16**, 303–306
- Jackson, R. S., Creemers, J. W., Farooqi, I. S., Raffin-Sanson, M. L., Varro, A., Dockray, G. J., Holst, J. J., Brubaker, P. L., Corvol, P., Polonsky, K. S., Ostrega, D., Becker, K. L., Bertagna, X., Hutton, J. C., White, A., Dattani, M. T., Hussain, K., Middleton, S. J., Nicole, T. M., Milla, P. J., Lindley, K. J., and O'Rahilly, S. (2003) *J. Clin. Investig.* **112**, 1550–1560
- Abifadel, M., Varret, M., Rabes, J. P., Allard, D., Ouguerram, K., Devillers, M., Cruaud, C., Benjannet, S., Wickham, L., Erlich, D., Derre, A., Villegier, L., Farnier, M., Beucher, I., Bruckert, E., Chambaz, J., Chanu, B., Lecerf, J. M., Luc, G., Moulin, P., Weissenbach, J., Prat, A., Krempf, M., Junien, C., Seidah, N. G., and Boileau, C. (2003) *Nat. Genet.* **34**, 154–156
- Rader, D. J., Cohen, J., and Hobbs, H. H. (2003) *J. Clin. Investig.* **111**, 1795–1803
- Timms, K. M., Wagner, S., Samuels, M. E., Forbey, K., Goldfine, H., Jammulapati, S., Skolnick, M. H., Hopkins, P. N., Hunt, S. C., and Shattuck, D. M. (2004) *Hum. Genet.* **114**, 349–353
- Leren, T. P. (2004) *Clin. Genet.* **65**, 419–422
- Shioji, K., Mannami, T., Kokubo, Y., Inamoto, N., Takagi, S., Goto, Y., Nonogi, H., and Iwai, N. (2004) *J. Hum. Genet.* **49**, 109–114
- Horton, J. D., Shah, N. A., Warrington, J. A., Anderson, N. N., Park, S. W., Brown, M. S., and Goldstein, J. L. (2003) *Proc. Natl. Acad. Sci. U. S. A.* **100**, 12027–12032
- Maxwell, K. N., Soccio, R. E., Duncan, E. M., Sehayek, E., and Breslow, J. L. (2003) *J. Lipid Res.* **44**, 2109–2119
- Dubuc, G., Chamberland, A., Wassef, H., Davignon, J., Seidah, N. G., Bernier, L., and Prat, A. (2004) *Arterioscler. Thromb. Vasc. Biol.* **24**, 1454–1459
- Sakai, J., Nohturfft, A., Goldstein, J. L., and Brown, M. S. (1998) *J. Biol. Chem.* **273**, 5785–5793
- Brown, M. S., and Goldstein, J. L. (1999) *Proc. Natl. Acad. Sci. U. S. A.* **96**, 11041–11048
- Bergeron, E., Basak, A., Decroly, E., and Seidah, N. G. (2003) *Biochem. J.* **373**, 475–484
- Conesa, M., Prat, A., Mort, J. S., Marvaldi, J., Lissitzky, J. C., and Seidah, N. G. (2003) *Biochem. J.* **370**, 703–711
- Benjannet, S., Elagoz, A., Wickham, L., Mamarbachi, M., Munzer, J. S., Basak, A., Lazure, C., Cromlish, J. A., Sisodia, S., Checler, F., Chretien, M., and Seidah, N. G. (2001) *J. Biol. Chem.* **276**, 10879–10887
- Louie, L. G., and King, M. C. (1991) *Am. J. Hum. Genet.* **48**, 637–638
- Goldstein, J. L., Basu, S. K., and Brown, M. S. (1983) *Methods Enzymol.* **98**, 241–260
- Yoshimura, A., Yoshida, T., Seguchi, T., Waki, M., Ono, M., and Kuwano, M. (1987) *J. Biol. Chem.* **262**, 13299–13308
- Hatch, F. T. (1968) *Adv. Lipid Res.* **6**, 1–68
- Brissette, L., Charest, M. C., and Falstra, L. (1996) *Biochem. J.* **318**, 841–847
- Langer, T., Strober, W., and Levy, R. I. (1972) *J. Clin. Investig.* **51**, 1528–1536
- Lowry, O. H., Rosebrough, N. J., Farr, A. L., and Randall, R. J. (1951) *J. Biol. Chem.* **193**, 265–275
- Hopkins, C. R., and Trowbridge, I. S. (1983) *J. Cell Biol.* **97**, 508–521
- Jin, W., Millar, J. S., Broedl, U., Glick, J. M., and Rader, D. J. (2003) *J. Clin. Investig.* **111**, 357–362
- Gluschankof, P., and Fuller, R. S. (1994) *EMBO J.* **13**, 2280–2288
- Elagoz, A., Benjannet, S., Mamarbachi, A., Wickham, L., and Seidah, N. G. (2002) *J. Biol. Chem.* **277**, 11265–11275
- Reed, P. W., and Lardy, H. A. (1972) *J. Biol. Chem.* **247**, 6970–6977
- Brayden, D. J., Hanley, M. R., Thastrup, O., and Cuthbert, A. W. (1989) *Br. J. Pharmacol.* **98**, 809–816
- Thyberg, J., and Moskalewski, S. (1985) *Exp. Cell Res.* **159**, 1–16
- Hortin, G., Polz, R., Gordon, J. I., and Strauss, A. W. (1986) *Biochem. Biophys. Res. Commun.* **141**, 326–333
- Beisswanger, R., Corbeil, D., Vannier, C., Thiele, C., Dohrmann, U., Kellner, R., Ashman, K., Niehrs, C., and Huttner, W. B. (1998) *Proc. Natl. Acad. Sci. U. S. A.* **95**, 11134–11139
- Ouguerram, K., Chetiveaux, M., Zair, Y., Costet, P., Abifadel, M., Varret, M., Boileau, C., Magot, T., and Krempf, M. (2004) *Arterioscler. Thromb. Vasc. Biol.* **8**, 1448–1453
- King-Underwood, L., Gudnason, V., Humphries, S., Seed, M., Patel, D., Knight, B., and Soutar, A. (1991) *Clin. Genet.* **40**, 17–28
- Gekle, M., Mildenerberger, S., Freudinger, R., and Silbernagl, S. (1995) *Am. J. Physiol.* **268**, F899–F906
- Kopfler, W. P., Willard, M., Betz, T., Willard, J. E., Gerard, R. D., and Meidell, R. S. (1994) *Circulation* **90**, 1319–1327
- Krieger, M. (1983) *Cell* **33**, 413–422
- Seidah, N. G. (2001) in *The Enzymes: Co- and Post-translational Proteolysis of Proteins* (Dalbey, R. E., and Sigman, D. S., eds) pp. 237–258, Academic

- Press, San Diego
49. Henrich, S., Cameron, A., Bourenkov, G. P., Kiefersauer, R., Huber, R., Lindberg, I., Bode, W., and Than, M. E. (2003) *Nat. Struct. Biol.* **10**, 520–526
  50. Zhou, A., Martin, S., Lipkind, G., LaMendola, J., and Steiner, D. F. (1998) *J. Biol. Chem.* **273**, 11107–11114
  51. Benjannet, S., Rondeau, N., Paquet, L., Boudreault, A., Lazure, C., Chretien, M., and Seidah, N. G. (1993) *Biochem. J.* **294**, 735–743
  52. De Bie, I., Marcinkiewicz, M., Malide, D., Lazure, C., Nakayama, K., Bendayan, M., and Seidah, N. G. (1996) *J. Cell Biol.* **135**, 1261–1275
  53. Gregersen, N., Bross, P., Andrese, B. S., Pedersen, C. B., Corydon, T. J., and Bolund, L. (2001) *J. Inherited Metab. Dis.* **24**, 189–212
  54. Siezen, R. J., and Leunissen, J. A. (1997) *Protein Sci.* **6**, 501–523
  55. Soutar, A. K. (1992) *J. Intern. Med.* **231**, 633–641
  56. Kunst, C. B., Mezey, E., Brownstein, M. J., and Patterson, D. (1997) *Nat. Genet.* **15**, 91–94
  57. Michaely, P., Li, W. P., Anderson, R. G., Cohen, J. C., and Hobbs, H. H. (2004) *J. Biol. Chem.* **279**, 34023–34031
  58. Twisk, J., Gillian-Daniel, D. L., Tebon, A., Wang, L., Barrett, P. H., and Attie, A. D. (2000) *J. Clin. Investig.* **105**, 521–532
  59. Tremblay, A. J., Lamarche, B., Ruel, I. L., Hogue, J. C., Bergeron, J., Gagne, C., and Couture, P. (2004) *J. Lipid Res.* **45**, 866–872
  60. Wang, L., Fast, D. G., and Attie, A. D. (1997) *J. Biol. Chem.* **272**, 27644–27651
  61. Maxwell, K. N., and Breslow, J. L. (2004) *Proc. Natl. Acad. Sci. U. S. A.* **101**, 7100–7105
  62. Varret, M., Rabes, J. P., Saint-Jore, B., Cenarro, A., Marinoni, J. C., Civeira, F., Devillers, M., Krempf, M., Coulon, M., Thiart, R., Kotze, M. J., Schmidt, H., Buzzi, J. C., Kostner, G. M., Bertolini, S., Pocovi, M., Rosa, A., Farnier, M., Martinez, M., Junien, C., and Boileau, C. (1999) *Am. J. Hum. Genet.* **64**, 1378–1387